



1 **Can Semi-Volatile Organic Aerosols Lead to Less Cloud Particles?**

2 **Chloe Y. Gao^{1,2}, Susanne E. Bauer², and Kostas Tsigaridis^{3,2}**

3 ¹Department of Earth and Environmental Sciences, Columbia University, New York, NY, 10027,
4 USA

5 ²NASA Goddard Institute for Space Studies, New York, NY, 10025, USA

6 ³Center for Climate Systems Research, Columbia University, New York, NY, 10025, USA

7

8 *Correspondence to:* Kostas Tsigaridis (kostas.tsigaridis@columbia.edu)

9

10 **Abstract.** The impact of condensing organic aerosols on activated cloud number concentration is
11 examined in a new aerosol microphysics box model, MATRIX-VBS. The model includes the
12 volatility-basis set (VBS) framework coupled with the aerosol microphysical scheme MATRIX
13 (Multiconfiguration Aerosol TRacker of mIXing state) that resolves aerosol mass and number
14 concentrations and aerosol mixing state. By including the condensation of organic aerosols, the
15 new model produces less activated particles compared to the original model, which treats organic
16 aerosols as non-volatile. Parameters such as aerosol chemical composition, mass and number
17 concentrations, and particle sizes which affect activated cloud number concentration are
18 thoroughly tested via a suite of Monte-Carlo simulations. Results show that by considering semi-
19 volatile organics in MATRIX-VBS, there is lower activated particle number concentration, except
20 in cases with low cloud updrafts, in clean environment at above freezing temperatures, and in
21 polluted environments at high temperature (310K) and extremely low humidity conditions.

22 **1 Introduction**

23 Atmospheric aerosols influence climate mainly via two pathways: aerosol-radiation
24 interactions (the aerosol direct effect; Charlson et al., 1992) which affect the Earth's radiative
25 energy balance by absorbing and scattering terrestrial and solar radiation, and aerosol-cloud
26 interactions (the aerosol indirect effect; Twomey, 1974; Albrecht, 1989) which affect cloud
27 microphysics by activating and serving as seeds for cloud formation (Myhre et al., 2013; Seinfeld
28 and Pandis, 2016). Aerosol activation as cloud condensation nuclei (CCN) is critical to the
29 evolution and microphysics of clouds (Reutter et al., 2009). However, the relationship between
30 aerosol mixing state and cloud microphysical properties remain a large uncertainty in aerosol-



31 cloud interactions (Ghan et al., 1998; McFiggans et al., 2006; Ervens et al., 2007; Gibson et al.,
32 2007; Medina et al., 2007; Cubison et al., 2008; Anttila, 2010).

33 Climate models calculate cloud droplet number concentration (CDNC) using aerosol
34 activation schemes, whose main governing parameters include aerosol number, size,
35 hygroscopicity, updraft velocity, as well as critical supersaturation. Physically-based aerosol
36 activation schemes (e.g. Abdul-Razzak and Ghan, 2000; Fountoukis and Nenes, 2005; Ming et al.,
37 2006; Shipway and Abel, 2010) are commonly used in global climate models for fast diagnostics
38 of nucleation and to estimate the aerosol indirect effect in long-term climate simulations (Ghan,
39 2011). Several studies examined the relationship between the fore-mentioned parameters and how
40 they play together to activate particles. Ghan et al. (1998) examined sea salt's influence on sulfate
41 particle activation and introduced the competition effect. Since all CCN have to compete for
42 available water vapor in order to activate, the competition limits the maximum supersaturation in
43 in-cloud updrafts (Storelvmo et al., 2006). Ghan et al. (1998) concluded that activated number
44 concentration increases with increasing sea salt when sulfate is low and updraft is strong, and it
45 decreases when sulfate is high and updraft is weak, because maximum supersaturation is reduced.
46 Another study (Reutter et al. 2009) explored how much CDNC depend on updraft velocity, size
47 distribution and hygroscopicity. They found that size distribution played a greater role than particle
48 hygroscopicity on CDNC and discovered different CCN activation and cloud droplet formation
49 regimes, which are determined by aerosol number concentration and updraft velocity.

50 Semi-volatile organic aerosols contribute significantly to the growth of particles to CCN
51 sizes (Yu, 2011). More notably, as aerosol size increases, the range of organic volatilities involved
52 in aerosol growth increases (Pierce et al., 2011; Yu, 2011). The inclusion of semi-volatile organics
53 in models modifies CCN formation rates (Petters et al., 2006, Riipinen et al., 2011; Scott et al.,
54 2015) as well as hygroscopicity (Petters and Kreidenweis, 2007), in addition to bulk aerosol mass,
55 size distribution and composition. By adding semi-volatile organic partitioning to our existing
56 microphysics model MATRIX (Multiconfiguration Aerosol TRacker of mIXing state; Bauer et al.,
57 2008), which resolves aerosol mixing state, we were able to examine how they change bulk aerosol
58 mass, size distribution and composition. However, the effects of semi-volatile organic partitioning
59 combined with aerosol mixing state on particle activation remain unexplored.

60 In our previous work, we demonstrated that including semi-volatile organics would lead to
61 higher aerosol number concentration and smaller particles (Gao et al., 2017). As was the case for



62 the original aerosol microphysics model MATRIX, our further-developed box model MATRIX-
63 VBS (Gao et al., 2017) follows the same multi-modal aerosol activation approach by Abdul-
64 Razzak and Ghan (2000). The activation parameterization accounts for aerosol size distribution,
65 composition, mixing state, and in-cloud updraft velocity. Curious about the change in activation
66 with the newly-present semi-volatile organics and the governing parameters influencing it, we
67 investigated the difference in activated number concentration in two box model set ups: MATRIX
68 (Bauer et al., 2008) and MATRIX-VBS (Gao et al., 2017).

69 2 Methods

70 2.1 Model Description

71 MATRIX-VBS (Gao et al., 2017) is an aerosol microphysics model that includes organic
72 aerosol volatility in its calculations. It was developed by implementing VBS (volatility-basis set;
73 Donahue et al., 2006) in the aerosol microphysics model MATRIX (Bauer et al., 2008), which is
74 a box model that is also used in the NASA GISS ModelE Earth System Model (Bauer et al., 2008,
75 2012; Schmidt et al., 2014). Since the publication of Gao et al., 2017, which included organic
76 condensation on fine mode aerosols, we further developed the model which now allows semi-
77 volatile organics in the system to condense on coarse mode dust and sea salt as well. We have also
78 included nitrate radicals as an oxidant for organics in addition to the hydroxyl radical that was used
79 in the original VBS scheme, even though it is a very minor oxidation pathway in the model (rate
80 constant for the oxidation by NO_3^{\cdot} is $1 \cdot 10^{-13} \text{ cm}^3 \text{ molecules}^{-1} \text{ s}^{-1}$; Atkinson, 1997). As previously
81 stated, we use Abdul-Razzak and Ghan (2000) activation parameterization, which calculates the
82 activated particle number concentration depending on chemically-resolved number concentrations
83 using Köhler Theory. The hygroscopicity parameters κ for each aerosol species presented in Table
84 1 were calculated from their solubility fraction. For organics, we assumed a linear increase of
85 solubility with decreasing volatility (Jimenez et al., 2009).

86 2.2 Simulations

87 A Monte-Carlo analysis with a range of chemical and meteorological conditions (Table 2)
88 was performed, to pinpoint which processes affect organics and the mixed aerosol population in
89 general the most. Since global models need to resolve a wide range of conditions, from very clean
90 to very polluted and for a wealth of meteorological conditions, we simulated 630 possible



91 atmospheric scenarios on Earth across the whole parameter space, e.g. temperature, relative
92 humidity, latitude, emissions levels and updraft velocity, for 120 hours (5 days) simulations with
93 no deposition and dilution. Three types of environmental conditions were simulated: clean,
94 moderate and polluted, as defined by different levels of emissions which were determined using a
95 probability distribution of the gridded emission fields in GISS ModelE for January present-day
96 conditions. During this development phase, biogenic secondary organic aerosols from terpenes
97 oxidation in MATRIX-VBS are treated as nonvolatile, while only the anthropogenic aerosols are
98 treated as semi-volatile.

99 **3 Results and discussion**

100 We found that activated number concentration is lower for most cases in the MATRIX-
101 VBS model, which considers semi-volatile organic aerosols, as compared to the MATRIX model.
102 However, under low updrafts, in clean environment at above freezing temperatures, and in polluted
103 environments at high temperature (310K) and extremely low humidity conditions (0% RH) during
104 aerosol formation, activated number concentration is higher in MATRIX-VBS than in MATRIX.

105 As an example, the activated number concentration for a case with temperature at 290°K,
106 relative humidity at 40%, medium emission levels and an updraft of 0.5 m/s at 30°N latitude is
107 shown in Figure 1 for the two models. Mixing states of aerosols in MATRIX and MATRIX-VBS
108 are represented as aerosol populations, which all contain SO₄, NO₃, NH₄ and H₂O, in addition to
109 the species that define the populations (Bauer et al., 2008, 2013). The four most dominant aerosol
110 populations for the activated number concentration in MATRIX are ACC (SO₄, NO₃, NH₄), OCS
111 (organics, SO₄, NO₃, NH₄), BOC (black carbon, organic carbon, SO₄, NO₃, NH₄) and BCS (black
112 carbon, SO₄, NO₃, NH₄). Only two dominant populations are calculated in MATRIX-VBS, OCS
113 and BOC, as in Gao et al., 2017, since OCC evaporates and re-condenses on all particles, based on
114 their calculated surface area and mass concentration. Since OCS and BOC have the largest surface
115 area, they are calculated to have the strongest growth via organics condensation. Additionally, the
116 competition between sulfate, organics and black carbon, determines the loss of ACC and the
117 formation of BCS: OCC coagulates with ACC to form OCS, and this coagulation increases in
118 MATRIX-VBS due to smaller OCC particles; therefore, there are less ACC particles left to
119 coagulate with black carbon to form BCS. At the end of the 5-day simulation (Figure 1), MATRIX-



120 VBS has approximately a total of 30 activated particles/cm³, whereas MATRIX has approximately
121 60 activated particles/cm³ under the same conditions.

122 Figure 2 shows a more comprehensive look across all temperature and relative humidity
123 scenarios studied. The results show that for most scenarios, MATRIX-VBS has lower (red circles)
124 activated number concentration compared to MATRIX. However, some rare cases show the
125 opposite behavior. These are for above freezing temperatures in the low emission level under low
126 updraft (top left) scenarios, high temperature (310K) and extremely low humidity (0% RH) in the
127 medium emission level under low updraft (middle left) scenarios, as well as the high emission
128 level under low (bottom left) and medium (bottom middle) updraft scenarios. Across all scenarios,
129 the changes in activated number concentration between MATRIX-VBS and MATRIX range from
130 a -56% to +31% (Table 3). The range of the difference becomes more significant as emission levels
131 increase, yet less significant as updraft velocity increases. Within most emission level-updraft
132 velocity scenarios, as temperature increases, the fractional change in activated number
133 concentration between the two models decreases. Also within most emission level-updraft velocity
134 scenarios (Figure 3, Table 4), as temperature increases, there are less activated particles in
135 MATRIX. We also observed the same behavior in MATRIX-VBS, higher temperature, less
136 activated particles.

137 In order to understand the cause of the difference in activation, we traced back to the key
138 difference between the two models: partitioning of organics. The inclusion of organics partitioning
139 leads to changes in aerosol mixing state and size distribution, as discussed in Gao et al. (2017).
140 Therefore, the change in activated number concentration could only be caused by changes in mass
141 concentration, number concentration and particle size. Since we use the Abdul-Razzak and Ghan
142 (2000) parameterization, and the activated number concentration is only a function of number
143 concentration and dry particle diameter.

144 As was the case in Gao et al., (2017), MATRIX-VBS has higher aerosol number
145 concentration (Figure 4 left) but smaller particles (Figure 4 right) compared to MATRIX in the
146 case presented in Figure 1. At first we expected that smaller particles would less likely activate, so
147 we performed a simple sensitivity test to confirm it. By changing dry particle diameter of the
148 particles in the activation scheme, the decreasing dry particle diameter indeed led to lower
149 activated number concentration. However, a second sensitivity test with changing only number



150 concentration showed that higher number concentration would actually lead to lower activated
151 number concentration as well.

152 In the Abdul-Razzak and Ghan (2000) scheme, increasing number concentration decreases
153 critical supersaturation, and lower critical supersaturation leads to higher minimum dry particle
154 radius that is able to activate. Therefore, activation is suppressed, since less particles exceed the
155 threshold radius. The activated number concentration is calculated from the activation fraction and
156 the number concentration. When the fraction is greater than the increase in number concentration,
157 lower activated number concentration is achieved, as shown here.

158 As mentioned previously, within most of the scenarios, there is a decrease in fractional
159 change as temperature increases, while both models experience decrease in activated number
160 concentration with increased temperature. This means the decrease in activated number
161 concentration for MATRIX-VBS is not as significant as that for MATRIX. There are two factors
162 that contribute to such change. First, the heat and moisture diffusion term is dependent on
163 temperature in the activation scheme (Abdul-Razzak and Ghan, 2000). Second, volatility of
164 organics is temperature dependent. In MATRIX-VBS, when organic volatility is considered, the
165 change is dampened. In other words, its number of activated particles is less sensitive to
166 temperature change as compared to MATRIX, leading to what we see in the circle plots that the
167 greater change at lower temperatures.

168 The length of day and season changes the duration and intensity of gas phase oxidation of
169 semi-volatile gases, which is why we also looked at aerosol evolution driven by photochemistry
170 at different latitudes. Since the model uses January emissions, different seasons are simulated at
171 the different hemispheres, while different day lengths are simulated at higher latitudes of the
172 southern hemisphere compared to tropical and high latitude northern hemisphere ones. As we
173 inspected results across latitudes in the two hemispheres, we found varying activated number
174 concentration in MATRIX-VBS compared to MATRIX and observed no evident trend. Such
175 inconclusive and complex results may be due to gas-phase chemistry and photochemical ageing
176 of semi-volatile organic vapors, which would require further examination in a separate dedicated
177 study.



178 4 Conclusions

179 With the inclusion of organic partitioning in an aerosol microphysics model, activated
180 aerosol number concentration is decreased under most temperature and relative humidity
181 conditions, except when under low updrafts, in clean environments at most temperatures and
182 relative humidities, and in polluted environments at high temperatures and extremely low humidity
183 conditions. Such changes are due to increased aerosol number concentration and smaller particles
184 in the new model, as well as how number concentration and size are calculated in the chosen
185 aerosol activation scheme, which determines how many particles are activated. Additionally, the
186 temperature dependence of activated number concentration is decreased for most scenarios.

187 The simulations in this study, however comprehensive, are still highly idealized. In fact,
188 Topping et al. (2013) showed that co-condensing organics lead to enhanced cloud droplet number
189 concentration, which seems to contradict our results. However, it is important to note that our study
190 is performed in a box model that does not resolve cloud physics. Activated number concentration
191 is a precursor for CDNC, whose actual numbers will depend on the cloud microphysical
192 calculation, which is not part of this study. We will investigate the effects of condensing organics
193 in a global climate model in the future. The results presented here implicate that in the new model,
194 most areas on Earth would experience less CCN on a typical day, but clean environments with
195 above freezing temperatures, or polluted environments on an extremely dry and hot day, would
196 form more CCN under low updraft velocity conditions, as compared to the old model. We expect
197 that implementing the improved box model in the global scale that includes a two moment cloud
198 microphysical scheme (Morrison and Gettelman, 2008; Gettelman and Morrison, 2015) would
199 more accurately represent aerosol-cloud interactions, which will be our focus on a follow up study.
200 Thus it would offer us valuable insights on how the addition of organic partitioning would change
201 cloud activation in the global atmosphere and its implications for climate.

202 **Acknowledgements.** We thank the NASA Earth and Space Science Fellowship Program (17-
203 EARTH17F-85) and the NASA Modeling, Analysis, and Prediction Program for supporting Chloe
204 Y. Gao's graduate study, as well as the NASA Atmospheric Composition Modeling and Analysis



205 Program (NNX15AE36G) for supporting Dr. Susanne E. Bauer and Dr. Kostas Tsigaridis. We also
206 thank Dr. Steven Ghan, Dr. Hyunho Lee and Dr. Ann Fridlind for sharing their insights with us.

207 The GISS ModelE Earth system model is publicly available. The box model code used here is
208 available upon request and will be publicly available in the future as part of GISS ModelE. The
209 data from all model simulations will be available upon request.

210 The authors declare that they have no conflict of interest.



211 **References**

- 212 Abdul-Razzak, H. and Ghan, S. J.: A parameterization of aerosol activation: 2. Multiple aerosol
213 types, *J. Geophys. Res. Atmospheres*, 105(D5), 6837–6844, doi:10.1029/1999JD901161, 2000.
214
- 215 Albrecht, B. A.: Aerosols, cloud microphysics, and fractional cloudiness, *Science*, 245, 1227–
216 1230, 1989.
217
- 218 Anttila, T.: Sensitivity of cloud droplet formation to the numerical treatment of the particle
219 mixing state, *J. Geophys. Res.*, 115, D21205, doi:10.1029/2010JD013995, 2010.
220
- 221 Atkinson, R.: Gas-phase tropospheric chemistry of volatile organic compounds: 1. Alkanes and
222 alkenes, *J. Phys. Chem. Ref. Data*, 26, 215–290, 1997.
223
- 224 Bauer, S. E., Wright, D. L., Koch, D., Lewis, E. R., McGraw, R., Chang, L.-S., Schwartz, S. E.,
225 and Ruedy, R.: MATRIX (Multiconfiguration Aerosol TRacker of mIXing state): an aerosol
226 microphysical module for global atmospheric models, *Atmos. Chem. Phys.*, 8, 6003–6035,
227 doi:10.5194/acp-8-6003-2008, 2008.
228
- 229 Bauer, S. E., and Menon, S.: Aerosol direct, indirect, semidirect, and surface albedo effects from
230 sector contributions based on the IPCC AR5 emissions for preindustrial and present-day
231 conditions, *J. Geophys. Res.*, 117, D01206, doi:10.1029/2011JD016816, 2012.
232
- 233 Bauer, S. E., Ault, A., and Prather, K. A.: Evaluation of aerosol mixing state classes in the GISS
234 modelE-MATRIX climate model using single-particle mass spectrometry measurements, *J.*
235 *Geophys. Res. Atmos.*, 118, 9834–9844, doi:10.1002/jgrd.50700, 2013.
236
- 237 Boucher, O., Randall, D., Artaxo, P., Bretherton, C., Feingold, G., Forster, P., Kerminen, V.-M.,
238 Kondo, Y., Liao, H., Lohmann, U., Rasch, P., Satheesh, S. K., Sherwood, S., Stevens, B., and
239 Zhang, X.-Y., Clouds and Aerosols, in: *Climate Change 2013: The Physical Science Basis,*
240 *Contribution of Working Group I to the Fifth Assessment Report of the Intergovernmental Panel*
241 *on Climate Change*, edited by: Stocker, T. F., Qin, D., Plattner, G.-K., Tignor, M., Allen, S. K.,



- 242 Boschung, J., Nauels, A., Xia, Y., Bex, V., and Midgley, P. M., Cambridge University Press,
243 Cambridge, UK and New York, NY, USA, 571–657, 2013.
244
- 245 Charlson, R. J., Schwartz, S. E., Hales, J. M., Cess, R. D., Coakley, J. A., Hansen, J. E., and
246 Hofmann, D. J.: Climate Forcing by Anthropogenic Aerosols, *Science*, 255, 423–430, 1992.
247
- 248 Cubison, M. J., Ervens, B., Feingold, G., Docherty, K. S., Ulbrich, I. M., Shields, L., Prather, K.,
249 Hering, S., and Jimenez, J. L.: The influence of chemical composition and mixing state of Los
250 Angeles urban aerosol on CCN number and cloud properties, *Atmos. Chem. Phys.*, 8, 5649–
251 5667, <https://doi.org/10.5194/acp-8-5649-2008>, 2008.
252
- 253 Donahue, N. M., Robinson, A. L., Stanier, C. O., and Pandis, S. N.: Coupled partitioning,
254 dilution, and chemical aging of semivolatile organics, *Environ. Sci. Technol.*, 40, 2635–2643,
255 doi:10.1021/es052297c, 2006.
256
- 257 Ervens, B., Cubison, M., Andrews, E., Feingold, G., Ogren, J. A., Jimenez, J. L., DeCarlo, P.,
258 and Nenes, A.: Prediction of cloud condensation nucleus number concentration using
259 measurements of aerosol size distributions and composition and light scattering enhancement
260 due to humidity, *J. Geophys. Res.*, 112, D10S32, doi:10.1029/2006jd007426, 2007.
261
- 262 Fountoukis, C. and Nenes, A.: Continued development of a cloud droplet formation
263 parameterization for global climate models, *J. Geophys. Res.*, 110, D11212,
264 doi:10.1029/2004JD005591, 2005.
265
- 266 Gao, C. Y., Tsigaridis, K., and Bauer, S. E.: MATRIX-VBS (v1.0): implementing an evolving
267 organic aerosol volatility in an aerosol microphysics model, *Geosci. Model Dev.*, 10, 751–764,
268 <https://doi.org/10.5194/gmd-10-751-2017>, 2017.
269
- 270 Gettelman, A. and Morrison, H.: Advanced Two-Moment Bulk Microphysics for Global Models,
271 Part I: Off-Line Tests and Comparison with Other Schemes, *J. Climate*, 28, 1268–1287,
272 <https://doi.org/10.1175/JCLI-D-14-00102.1>, 2015.



273

274 Ghan, S. J., Abdul-Razzak, H., Nenes, A., Ming, Y., Liu, X., Ovchinnikov, M., Shipway, B.,
275 Meskhidze, N., Xu, J., and Shi, X.: Droplet nucleation: physically-based parameterizations and
276 comparative evaluation, *J. Adv. Model. Earth Syst.*, 3, M10001, doi:10.1029/2011MS000074,
277 2011.

278

279 Ghan, S. J., Guzman, G., and Abdul-Razzak, H.: Competition between sea salt and sulfate
280 particles as cloud condensation nuclei, *Journal 25. of the atmospheric sciences*, 55, 3340-
281 3347, 1998.

282

283 Gibson, E.R., Gierlus, K.M., Hudson, P.K., Grassian, V.H.: Generation of internally mixed
284 insoluble and soluble aerosol particles to investigate the impact of atmospheric aging and
285 heterogeneous processing on the CCN activity of mineral dust aerosol, *Aerosol Sci. Technol.*, 41,
286 914–924, 2007.

287

288 Jimenez, J. L., Canagaratna, M. R., Donahue, N. M., Prevot, A. S. H., Zhang, Q., Kroll, J. H.,
289 DeCarlo, P. F., Allan, J. D., Coe, H., Ng, N. L., Aiken, A. C., Docherty, K. S., Ulbrich, I. M.,
290 Grieshop, A. P., Robinson, A. L., Duplissy, J., Smith, J. D., Wilson, K. R., Lanz, V. A., Hueglin,
291 C., Sun, Y. L., Tian, J., Laaksonen, a, Raatikainen, T., Rautiainen, J., Vaattovaara, P., Ehn, M.,
292 Kulmala, M., Tomlinson, J. M., Collins, D. R., Cubison, M. J., Dunlea, E. J., Huffman, J. A.,
293 Onasch, T. B., Alfarra, M. R., Williams, P. I., Bower, K., Kondo, Y., Schneider, J., Drewnick, F.,
294 Borrmann, S., Weimer, S., Demerjian, K., Salcedo, D., Cottrell, L., Griffin, R., Takami, A.,
295 Miyoshi, T., Hatakeyama, S., Shimono, A., Sun, J. Y., Zhang, Y. M., Dzepina, K., Kimmel, J.
296 R., Sueper, D., Jayne, J. T., Herndon, S. C., Trimborn, A. M., Williams, L. R., Wood, E. C.,
297 Middlebrook, A. M., Kolb, C. E., Baltensperger, U., and Worsnop, D. R.: Evolution of organic
298 aerosols in the atmosphere, *Science*, 326, 1525–1529, doi:10.1126/science.1180353, 2009.

299

300 McFiggans, G., et al. (2006), The effect of physical and chemical aerosol
301 properties on warm c loud dr oplet activation, *Atmos. Chem. Phys.*, 6,
302 2593–2649.

303



- 304 McFiggans, G., Artaxo, P., Baltensperger, U., Coe, H., Facchini, M. C., Feingold, G., Fuzzi, S.,
305 Gysel, M., Laaksonen, A., Lohmann, U., Mentel, T. F., Murphy, D. M., O'Dowd, C. D., Snider,
306 J. R., and Weingartner, E.: The effect of physical and chemical aerosol properties on warm cloud
307 droplet activation, *Atmos. Chem. Phys.*, 6, 2593-2649, <https://doi.org/10.5194/acp-6-2593-2006>,
308 2006.
309
- 310 Medina, J., Nenes, A., Sotiropoulou, R.-E. P., Cottrell, L. D., Ziemba, L. D., Beckman, P. J., and
311 Griffin, R. J.: Cloud condensation nuclei closure during the International Consortium for
312 Atmospheric Research on Transport and Transformation 2004 campaign: Effects of size-resolved
313 composition, *J. Geophys. Res.*, 112, D10S31, doi:10.1029/2006jd007588, 2007.
314
- 315 Ming, Y., Ramaswamy, V., Donner, L. J., and Phillips, V. T. J.: A new parameterization of cloud
316 droplet activation applicable to general circulation models, *J. Atmos. Sci.*, 63, 1348–1356, 2006.
317
- 318 Morrison, H. and Gettelman, A.: A new two-moment bulk stratiform cloud microphysics scheme
319 in the Community Atmosphere Model, version 3 (CAM3). Part I: Description and numerical
320 tests, *J. Climate*, 21, 3642–3659, <https://doi.org/10.1175/2008JCLI2105.1>, 2008.
321
- 322 Myhre, G., Shindell, D., Bréon, F.-M., Collins, W., Fuglestedt, J., Huang, J., Koch, D.,
323 Lamarque, J.-F., Lee, D., Mendoza, B., Nakajima, T., Robock, A., Stephens, G., Takemura T.,
324 and Zhang, H.: Anthropogenic and Natural Radiative Forcing, in: *Climate Change 2013: The*
325 *Physical Science Basis. Contribution of Working Group I to the Fifth Assessment Report of the*
326 *Intergovernmental Panel on Climate Change*, edited by: Stocker, T. F., Qin, D., Plattner, G.-K.,
327 Tignor, M., Allen, S. K., Boschung, J., Nauels, A., Xia, Y., Bex, V., and Midgley, P. M.,
328 Cambridge University Press, Cambridge, UK and New York, NY, USA, 659– 740,
329 doi:10.1017/CBO9781107415324, 2013.
330
- 331 Petters, M. D. and Kreidenweis, S. M.: A single parameter representation of hygroscopic growth
332 and cloud condensation nucleus activity, *Atmos. Chem. Phys.*, 7, 1961–1971, doi:10.5194/acp-7-
333 1961-2007, 2007.
334



- 335 Petters, M. D., Prenni, A. J., Kreidenweis, S. M., DeMott, P. J., Matsunaga, A., Lim, Y. B., and
336 Ziemann, P. J.: Chemical aging and the hydrophobic-hydrophilic conversion of carbonaceous
337 aerosol, *Geophys. Res. Lett.*, 33, L24806, doi:10.1029/2006GL027249, 2006.
338
- 339 Pierce, J. R., Riipinen, I., Kulmala, M., Ehn, M., Petäjä, T., Junninen, H., Worsnop, D. R., and
340 Donahue, N. M.: Quantification of the volatility of secondary organic compounds in ultrafine
341 particles during nucleation events, *Atmos. Chem. Phys.*, 11, 9019–9036, doi:10.5194/acp-11-
342 9019-2011, 2011.
343
- 344 Reutter, P., Su, H., Trentmann, J., Simmel, M., Rose, D., Gunthe, S. S., Wernli, H., Andreae, M.
345 O., and Pöschl, U.: Aerosol- and updraft-limited regimes of cloud droplet formation: influence of
346 particle number, size and hygroscopicity on the activation of cloud condensation nuclei (CCN),
347 *Atmos. Chem. Phys.*, 9, 7067-7080, <https://doi.org/10.5194/acp-9-7067-2009>, 2009.
348
- 349 Riipinen, I., Pierce, J. R., Yli-Juuti, T., Nieminen, T., Häkkinen, S., Ehn, M., Junninen, H.,
350 Lehtipalo, K., Petäjä, T., Slowik, J., Chang, R., Shantz, N. C., Abbatt, J., Leaitch, W. R.,
351 Kerminen, V.-M., Worsnop, D. R., Pandis, S. N., Donahue, N. M., and Kulmala, M.: Organic
352 condensation: a vital link connecting aerosol formation to cloud condensation nuclei (CCN)
353 concentrations, *Atmos. Chem. Phys.*, 11, 3865–3878, doi:10.5194/acp-11-3865-2011, 2011.
354
- 355 Schmidt, G. A., Kelley, M., Nazarenko, L., Ruedy, R., Russell, G. L., Aleinov, I., Bauer, M.,
356 Bauer, S. E., Bhat, M. K., Bleck, R., Canuto, V., Chen, Y., Cheng, Y., Clune, T. L., Del Genio,
357 A., de Fainchtein, R., Faluvegi, G., Hansen, J. E., Healy, R. J., Kiang, N. Y., Koch, D., Lacis, A.,
358 A., LeGrande, A. N., Lerner, J., Lo, K. K., Matthews, E. E., Menon, S., Miller, R. L., Oinas, V.,
359 Oloso, A. O., Perlwitz, J. P., Puma, M. J., Putman, W. M., Rind, D., Romanou, A., Sato, M.,
360 Shindell, D. T., Sun, S., Syed, R. A., Tausnev, N., Tsigaridis, K., Unger, N., Voulgarakis, A.,
361 Yao, M.-S., and Zhang, J.: Configuration and assessment of the GISS ModelE2 contributions to
362 the CMIP5 archive, *J. Adv. Model. Earth Syst.*, 6, 141–184, doi:10.1002/2013MS000265, 2014.
363
- 364 Scott, C. E., Spracklen, D. V., Pierce, J. R., Riipinen, I., D’Andrea, S. D., Rap, A., Carslaw, K.
365 S., Forster, P. M., Artaxo, P., Kulmala, M., Rizzo, L. V., Swietlicki, E., Mann, G. W., and



- 366 Pringle, K. J.: Impact of gas-to-particle partitioning approaches on the simulated radiative effects
367 of biogenic secondary organic aerosol, *Atmos. Chem. Phys.*, 15, 12989–13001, doi:10.5194/acp-
368 15- 12989-2015, 2015.
- 369
- 370 Seinfeld, J. H. and Pandis, S. N.: *Atmospheric Chemistry and Physics: From Air Pollution to*
371 *Climate Change*, third edition, John Wiley & Sons Inc., Hoboken, New Jersey, 2016.
- 372
- 373 Shipway, B. J. and Abel, S. J.: Analytical estimation of cloud droplet nucleation based on an
374 underlying aerosol population, *Atmos. Res.*, 96, 344–355, 2010.
- 375
- 376 Storelvmo, T., Kristjansson, J. E., Ghan, S. J., Kirkevåg, A., Seinfeld, Ø., and Iversen, J.:
377 Predicting cloud droplet number concentration in Community Atmosphere Model (CAM)-Oslo,
378 *J. Geophys. Res.*, 111, D24208, doi:10.1029/2005JD006300, 2006.
- 379
- 380 Topping, D., Connolly, P., and McFiggans, G.: Cloud droplet number enhanced by co-
381 condensation of organic vapours, *Nature Geosci.*, 6, 443–446, 2013.
- 382
- 383 Twomey, S. A.: Pollution and the Planetary albedo, *Atmos. Environ.*, 8, 1251–1256, 1974.
- 384
- 385 Yu, F.: A secondary organic aerosol formation model considering successive oxidation aging and
386 kinetic condensation of organic compounds: global scale implications, *Atmos. Chem. Phys.*, 11,
387 1083–1099, doi:10.5194/acp-11-1083-2011, 2011.
- 388

389 **Table 1. Hygroscopicity κ used for each organic aerosol volatility bin.**

	$\log_{10}C^*$ [$\mu\text{g m}^{-3}$]	soluble fraction [%]	κ
Sulfate	/	100	0.507
Black carbon	/	0	$5 \cdot 10^{-7}$
Non-volatile organic carbon	/	78	0.141
	-2	100	0.180
	-1	87.5	0.158
	0	75	0.135
Semi-volatile organic carbon	1	62.5	0.113
	2	50	0.090
	3	37.5	0.068
	4	25	0.045
	5	12.5	0.023
	6	0	0.000
Dust	/	13	0.14
Sea salt	/	100	1.335

390

391

392 **Table 2. Parameters used in the Monte-Carlo simulations.**

Parameter		Range	
	T [K]	270, 280, 290, 300, 310	
	RH [%]	0.1, 20, 40, 60, 80, 100	
	Latitude	0, 30N/S, 60N/S, 90N/S	
	Updraft velocity [m/s]	0.5, 1, 2	
Emissions of aerosols [$\mu\text{g}/\text{m}^3/\text{s}$]	Sulfate (SO_2 in molecules/ cm^3)	$10^5, 10^6, 5 \cdot 10^6$	
	Primary organics	$5 \cdot 10^{-6}, 5 \cdot 10^{-5}, 5 \cdot 10^{-4}$	
	Nonvolatile biogenic organics from terpene source	$1 \cdot 10^{-8}, 5 \cdot 10^{-6}, 1 \cdot 10^{-5}$	
	Black Carbon	$10^{-6}, 10^{-5}, 10^{-4}$	
Emissions of gases [molecules/ cm^3]	VOCs (in sets)	Alkenes	$5 \cdot 10^2, 5 \cdot 10^3, 5 \cdot 10^4$
		Paraffin	$5 \cdot 10^3, 10^4, 5 \cdot 10^4$
		Terpenes	$10^4, 10^5, 10^6$
		Isoprene	$10^4, 10^5, 50^6$
		NO_x	$10^5, 10^6, 10^7$

393

394



395 **Table 3. Minimum and maximum of fractional change in average activated number**
 396 **concentration over the last 24 hours between the two models with low, medium and high**
 397 **level emissions at updraft velocities of 0.5, 1 and 2 m/s.**

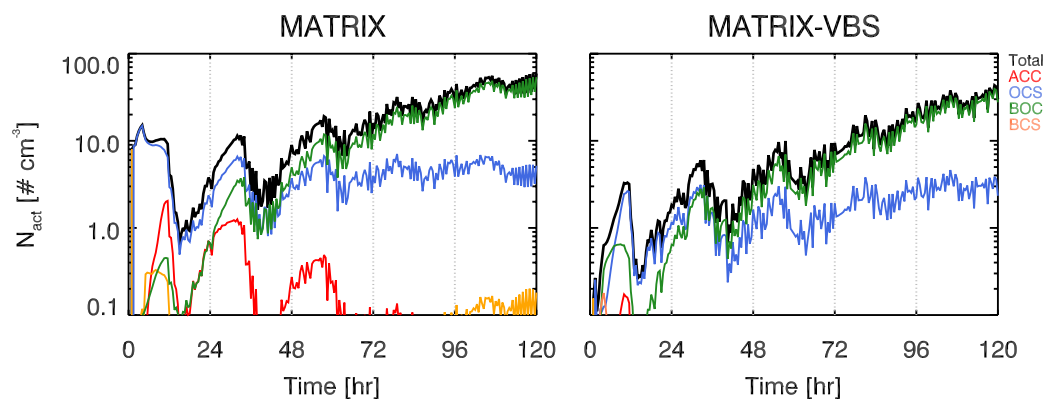
Updraft velocity (m/s)	Fractional change in activated number concentration					
	0.5		1		2	
	min	max	min	max	min	max
Low emission level	-9%	+21%	-16%	+2%	-14%	+5%
Medium emission level	-51%	+14%	-42%	-5%	-36%	-13%
High emission level	-56%	+31%	-48%	+9%	-43%	-9%

398

399

400 **Table 4. Minimum and maximum of average activated number concentration over the last**
 401 **24 hours of MATRIX and MATRIX-VBS with low, medium and high level emissions at**
 402 **updraft velocities of 0.5, 1 and 2 m/s.**

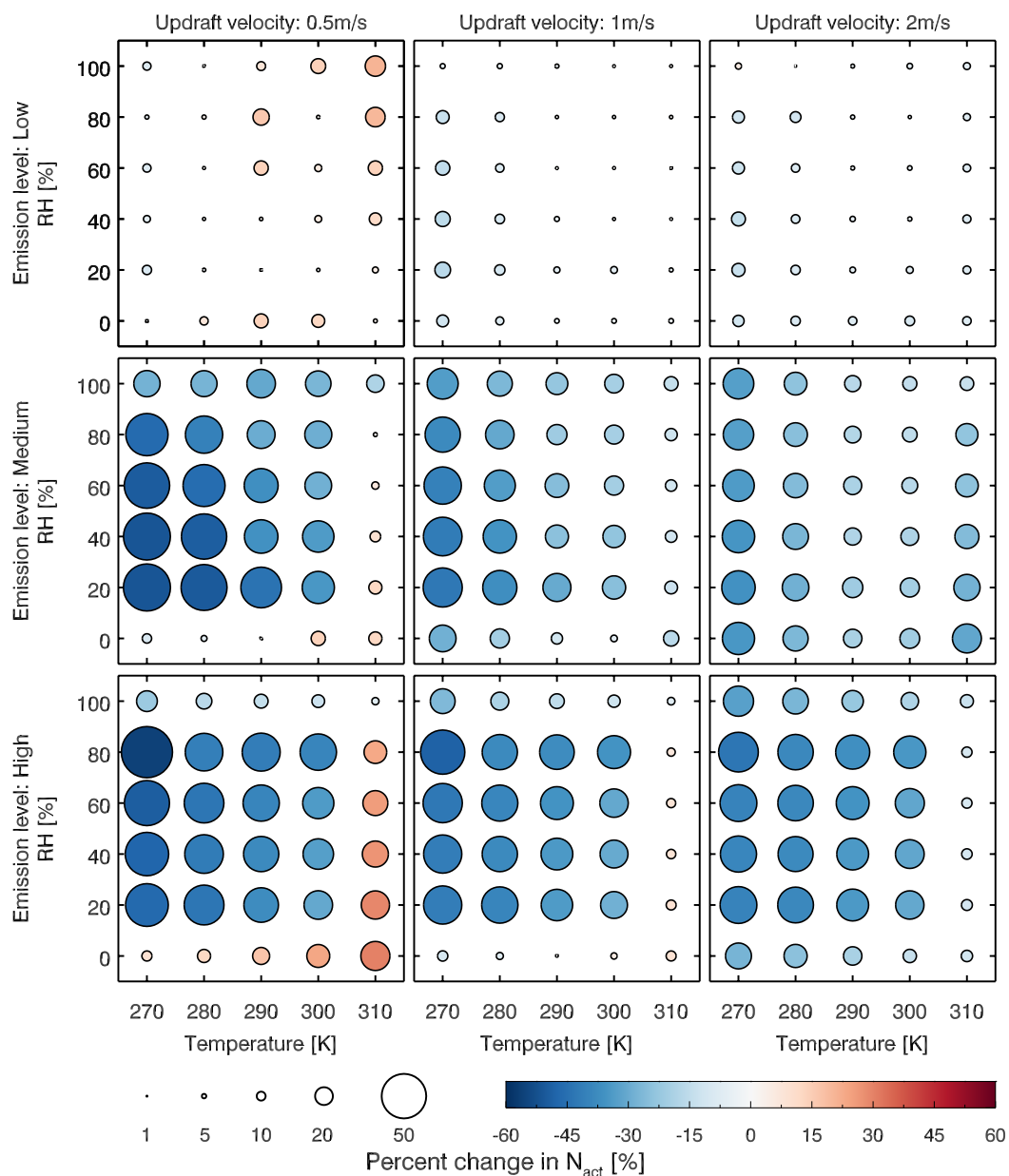
Updraft velocity (m/s)		Activated number concentration					
		0.5		1		2	
		min	max	min	max	min	max
Low emission level	MATRIX	23	305	351	1160	963	2799
	MATRIX-VBS	24	283	338	1026	887	2473
Medium emission level	MATRIX	19	152	359	1233	1476	3711
	MATRIX-VBS	16	139	304	884	1021	2498
High emission level	MATRIX	3	60	199	1280	1925	5703
	MATRIX-VBS	3	63	185	1150	1677	4142



403

404 **Figure 1. Activated number concentration of aerosol populations (see main text for details)**
405 **for MATRIX (left) and MATRIX-VBS (right) for 290 K and 40% RH at 30°N latitude with**
406 **medium emission levels and 0.5 m/s updraft velocity.**

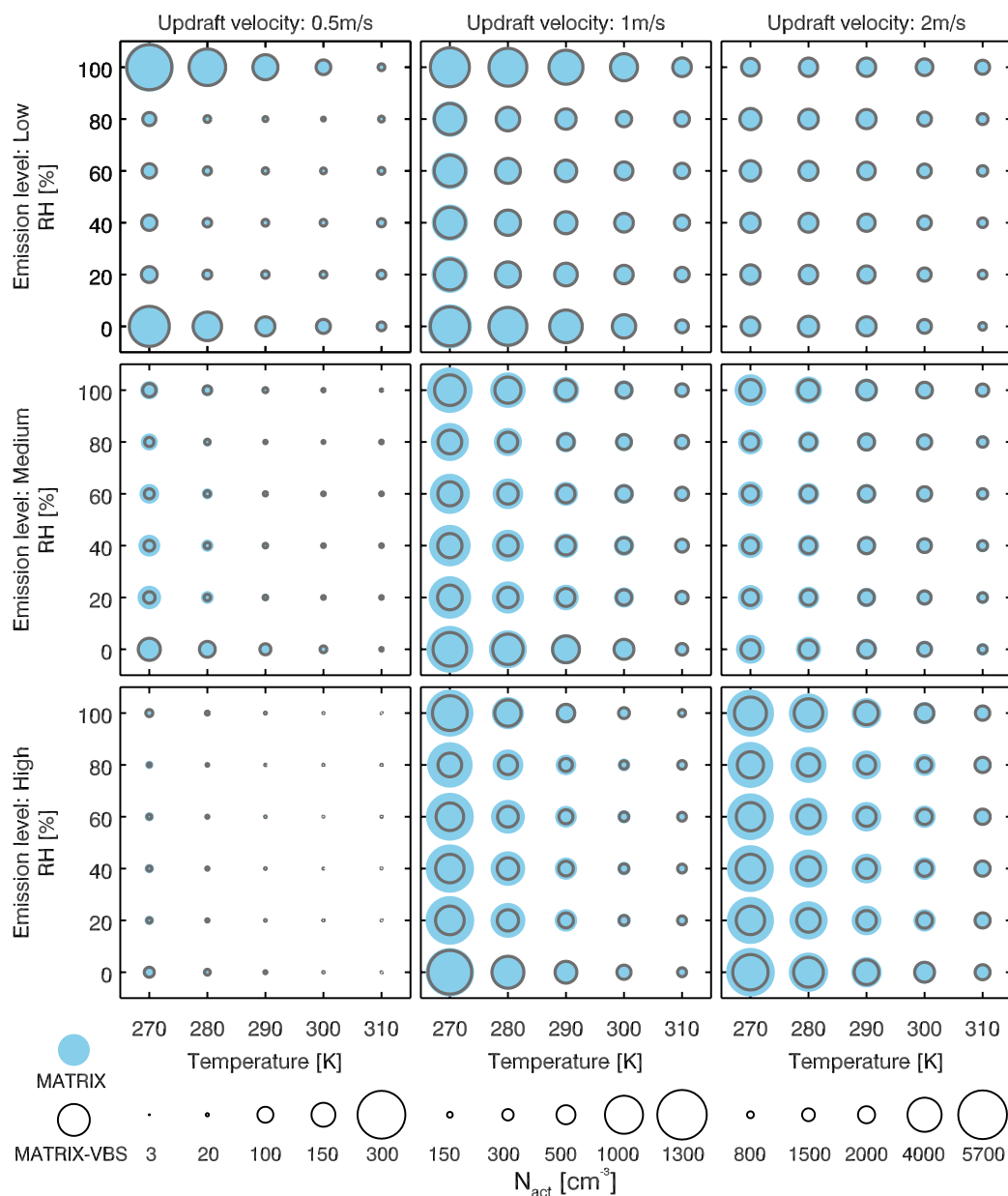
407



408

409 **Figure 2. Fractional change of average activated number concentration (size and color of the**
 410 **circles) over the last 24 hours of a 5-day simulation between the two models with low (top**
 411 **row), medium (middle row) and high (bottom row) level emissions at updraft velocities of 0.5**
 412 **(left column), 1 (middle column) and 2 (right column) m/s.**

413



414

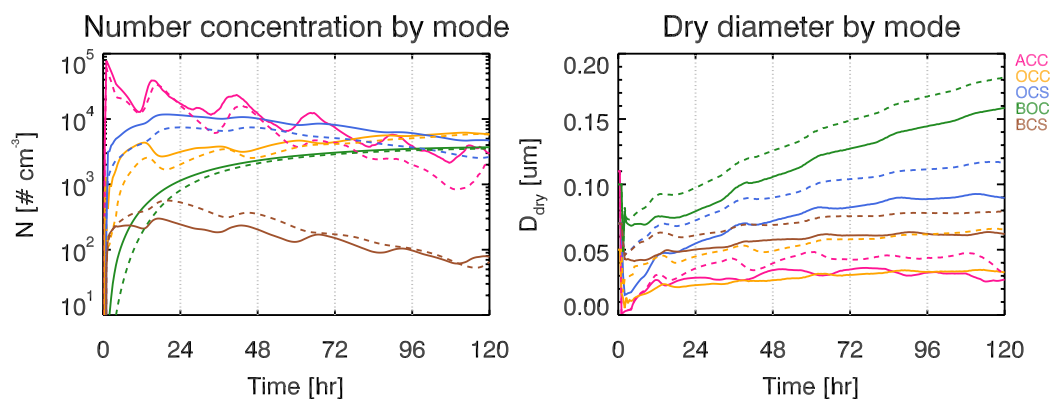
415

416 **Figure 3. Average activated number concentration (circle size) during the last 24 hours of a**

417 **5-day simulation in MATRIX and MATRIX-VBS with low (top row), medium (middle row)**

418 **and high (bottom row) emission levels at updraft velocities of 0.5 (left column), 1 (middle**

and 2 (right column) m/s. Note difference in scales per column.



419

420 **Figure 4. Number concentration (left column) and dry particle diameter (right column) by**
 421 **mode (color lines) for MATRIX (dashed lines) and MATRIX-VBS (solid lines) for the**
 422 **experiments with the same conditions as Figure 1.**